Electronic Supporting Information

Mechanical Deformation and Multiple Thermal Restoration of Organic Crystals: Reversible Multi-Stage Shape-Changing Effect with Luminescence-Color Changes

Chi Feng,[a] Tomohiro Seki,*[b] Shunichi Sakamoto,[c] Toshiyuki Sasaki,[c] Satoshi Takamizawa,*[c] and Hajime Ito*[a,d]

[a]Division of Applied Chemistry, Graduate School of Engineering, Hokkaido University, Sapporo, Hokkaido 060-8628, Japan

[b]Department of Chemistry, Faculty of Science, Shizuoka University, Shizuoka City, Shizuoka 422-8017, Japan

[c]Department of Materials System Science, Graduate School of Nanobioscience, Yohohama City University, 22-2 Seto, Kanazawa-ku, Yohohama, Kanagawa 236-0027, Japan

[d]Institute for Chemical Reaction Design and Discovery (WPI-ICReDD), Hokkaido University 060-8628, Japan

Email:
seki.tomohiro@shizuoka.ac.jp; staka@yokohama-cu.ac.jp; hajito@eng.hokudai.ac.jp

Contents

1. General

All commercially available reagents and solvents are of reagent grade and were used without further purification unless otherwise noted. Solvents for the synthesis were purchased from commercial suppliers, degassed by three freeze-pump-thaw cycles and further dried over molecular sieves (4 Å). NMR spectra were recorded on a JEOL JNM-ECX400P or JNM-ECS400 spectrometer (^{1}H: 392 MHz; ^{13}C: 98.5 MHz) using tetramethylsilane and $CDCl_3$ as internal standards, respectively. Emission spectra were measured by using an Olympus fluorescence microscope BX51 equipped with Hamamatsu photonics multichannel analyzer PM-12. The absorption spectra of the solid samples were recorded on a JASCO V-660 UV-VIS spectrophotometer. The emission quantum yields of the solid samples were recorded on a Hamamatsu Quantaurus-QY spectrometer with an integrating sphere. Emission lifetime measurements were recorded on a Hamamatsu Quantaurus-Tau spectrometer. Elemental analyses and high-resolution mass spectra were recorded at Global Facility Center, Creative Research Institution, Hokkaido University. Photographs were obtained using Olympus BX51 or SZX7 microscopes with Olympus DP72, or Sony $\alpha7_{SII}$ digital cameras. Scanning electron microscopic images were acquired by using JEOL JSM-6510LV. Stress-strain tests were carried out on a universal testing machine (Tensilon RTG-1210, A&D Co. Ltd.). Differential Scanning Calorimetry (DSC) profiles were measured on DSC Q2000 V24.11.

X-ray diffraction analyses: Single crystal X-ray structural analyses were carried out on a Rigaku XtaLAB PRO MM007 diffractometer using graphite monochromated Mo-K_α radiation. The structure was solved by direct methods and expanded using Fourier techniques. Non-hydrogen atoms were refined anisotropically. Hydrogen atoms were refined using the riding model. All calculations were performed using the Olex2 crystallographic software package except for refinement, which was performed using SHELXT-2018.[S1] The structures were solved by direct methods with (SHELXT)[S1] and refined by full-matrix least-squares techniques against F2 (SHELXL-2018/3)[S2] by using Olex2 software package.[S3]

2. Synthesis of 1

Scheme for the synthesis of **1.**

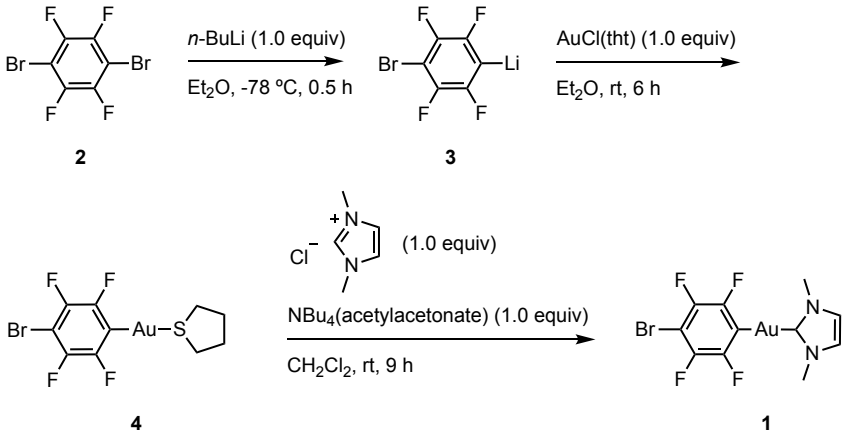

*Synthesis of 1-bromo-2,3,5,6-tetrafluorobenzenyl(1,3-dimethylimidazolin-2-ylidene)gold complex **1**.*

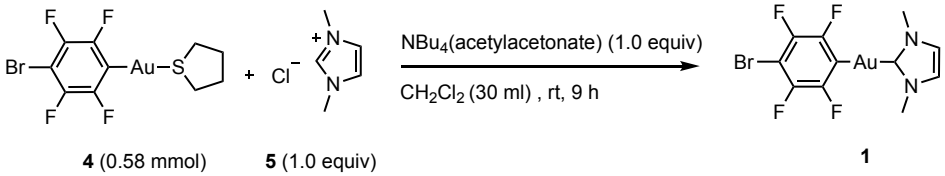

Compound **1** was prepared by the modification of the literature method.[S4] An oven-dried two-neck flask was connected to a vacuum/nitrogen manifold through a rubber tube. It was evacuated and then backfilled with nitrogen. This cycle was repeated three times. In this flask, **4**[S5] (297 mg, 0.58 mmol) and **5** (77 mg, 0.58 mmol) were dissolved in CH_2Cl_2 (30 ml) and stirred until a colorless solution formed (5 min). Then, NBu_4(acetylacetonate)[S4] (198 mg, 0.58 mmol) was added and stirred for 9 h at room temperature. The reaction mixture was directly filtered through a plug of silica and the colorless filtrate was evaporated to minimum volume. Hexane was added to the residue to form a white solid which was collected through the filtration and vacuum dried to give the analytically pure product **1** (118 mg, 0.23 mmol, 40%). ^{1}H NMR (392 MHz, $CDCl_3$, δ): 3.91 (s, 6H, Me), 6.94 (s, 2*H*, imidazole). ^{13}C NMR (98.5 MHz, $CDCl_3$, δ): 37.75 (s, Me), 94.30–94.77 (m, Br-*C*), 121.71 (s, *C*H, imidazole), 140.51–141.69 (m, Au-*C*-C), 142.90–145.73 (m, F-*C*), 148.49–151.19 (m, F-*C*), 188.74 (s, N-*C*-N). ESI-MS (*m*/*z*): $[M+Na]^+$ calcd for $C_{11}H_8AuBrF_4N_2Na$, 542.93702; found, 542.93697.

3. Preparation and images of the single crystals of 1

*Preparation of the single crystal of **1***:

The single crystal of **1** was obtained by liquid-liquid diffusion. Typically, **1** (50 mg) is dissolved in 2 mL of CH_2Cl_2 in a vial and hexane (6 mL) was carefully layered. After standing for 1 days at room temperature, the colorless single crystals of **1** were formed.

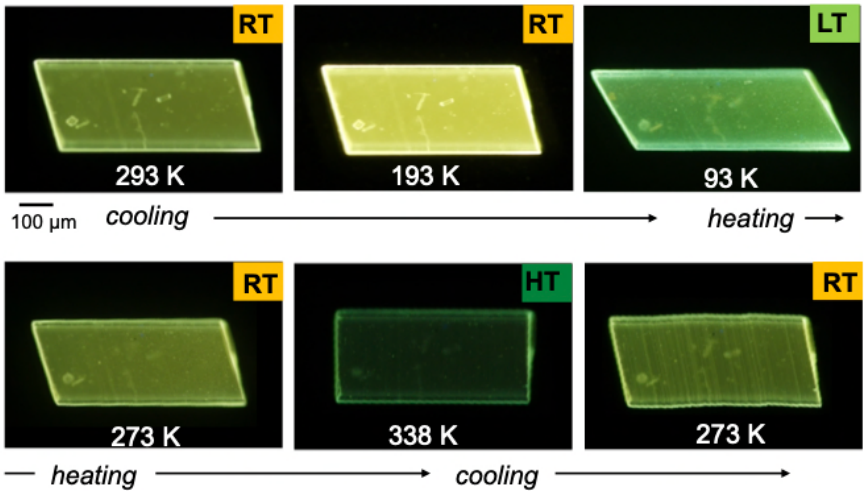

Fig. S1. Photographs of a crystal of **1** observed upon cooling/heating at 20 K min^{-1} under UV light.

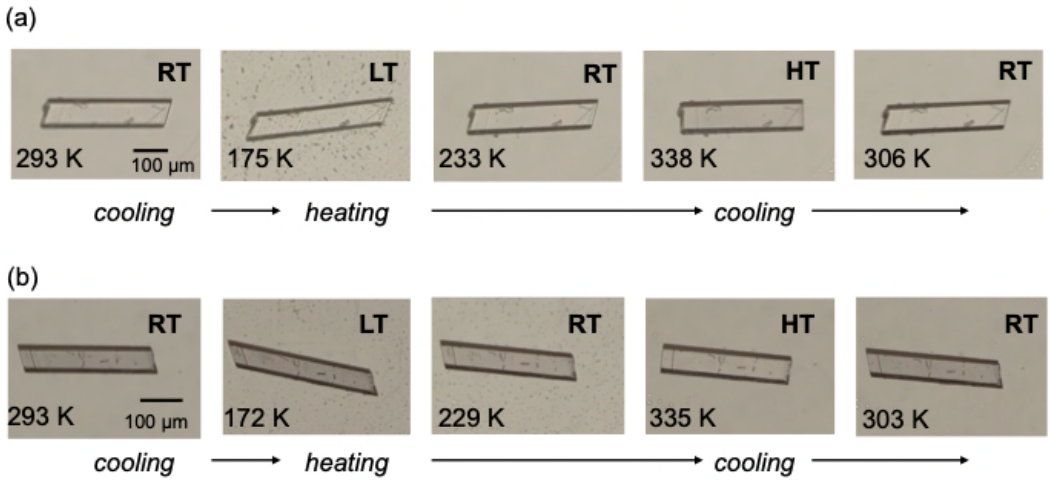

Fig. S2. Photographs of a crystal of **1** observed upon cooling/heating at 20 K min^{-1} under room light.

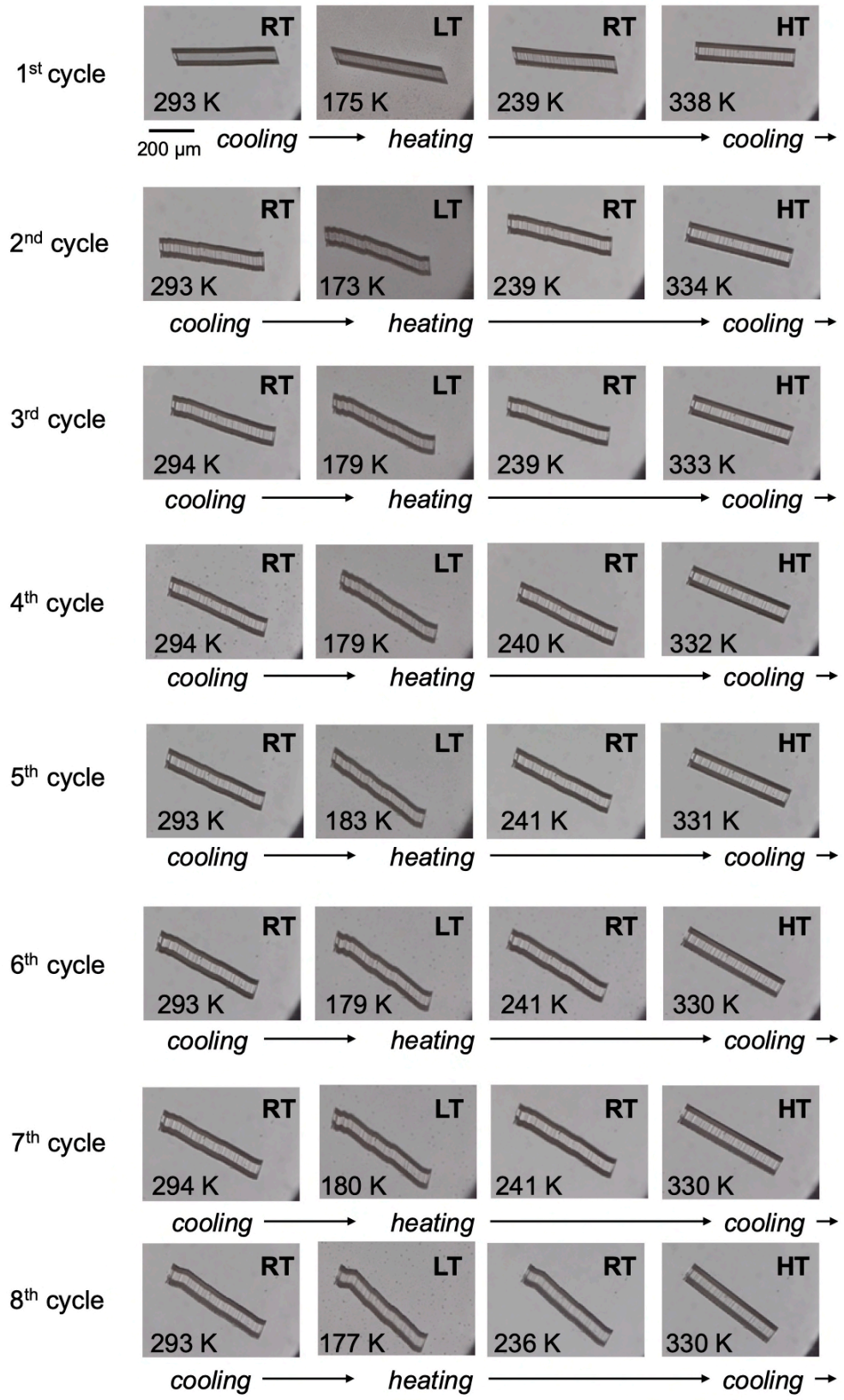
1st cycle
RT
293 K
LT
175 K
RT
239 K
HT
338 K
200 μm
cooling
heating
cooling
2nd cycle
RT
293 K
LT
173 K
RT
239 K
HT
334 K
cooling
heating
cooling
3rd cycle
RT
294 K
LT
179 K
RT
239 K
HT
333 K
cooling
heating
cooling
4th cycle
RT
294 K
LT
179 K
RT
240 K
HT
332 K
cooling
heating
cooling
5th cycle
RT
293 K
LT
183 K
RT
241 K
HT
331 K
cooling
heating
cooling
6th cycle
RT
293 K
LT
179 K
RT
241 K
HT
330 K
cooling
heating
cooling
7th cycle
RT
294 K
LT
180 K
RT
241 K
HT
330 K
cooling
heating
cooling
8th cycle
RT
293 K
LT
177 K
RT
236 K
HT
330 K
cooling
heating
cooling

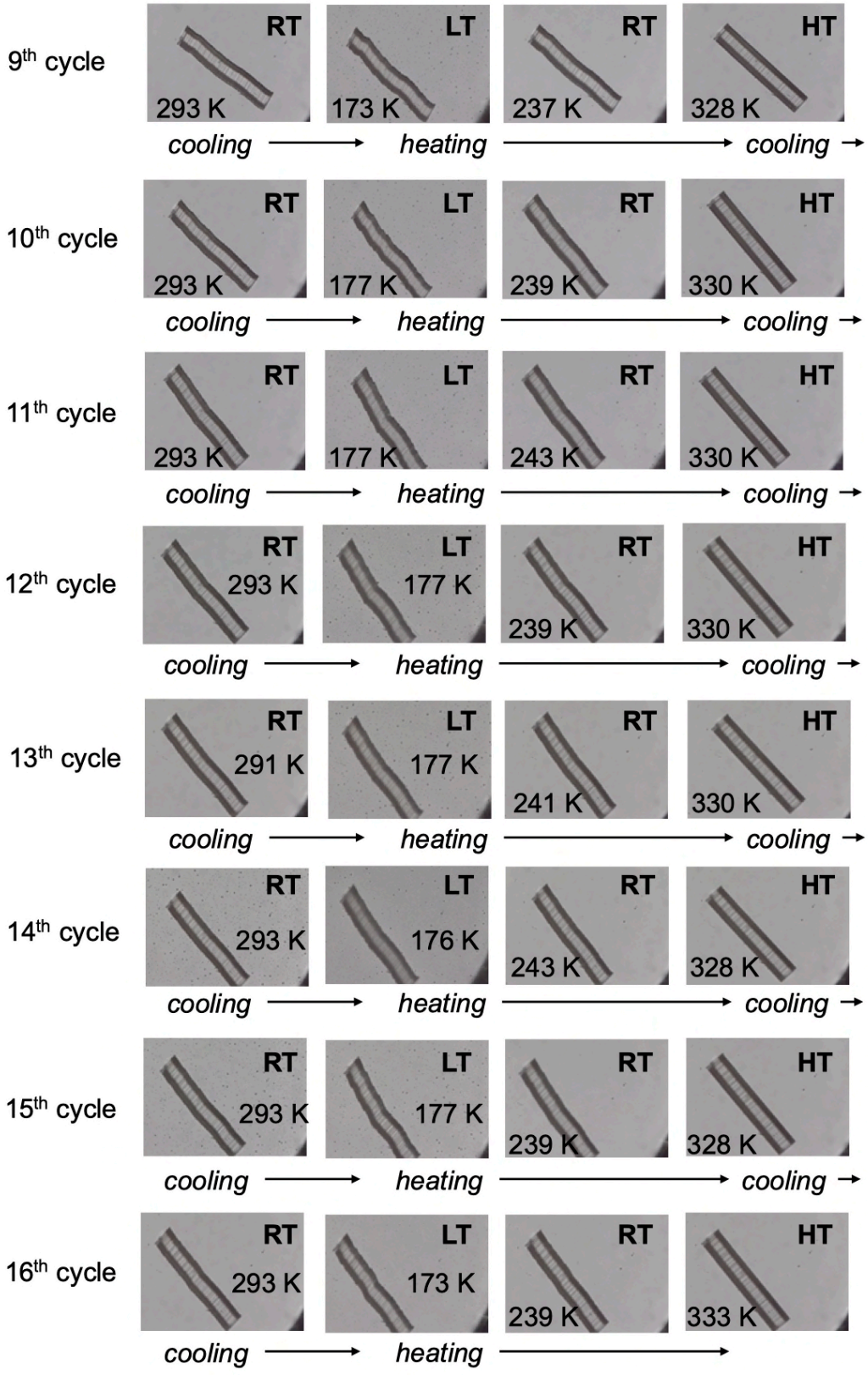

Fig. S3. Photographs of crystal **1** observed under room light upon heating/cooling at 20 K min^{-1}.

4. Differential scanning calorimetry profiles of 1

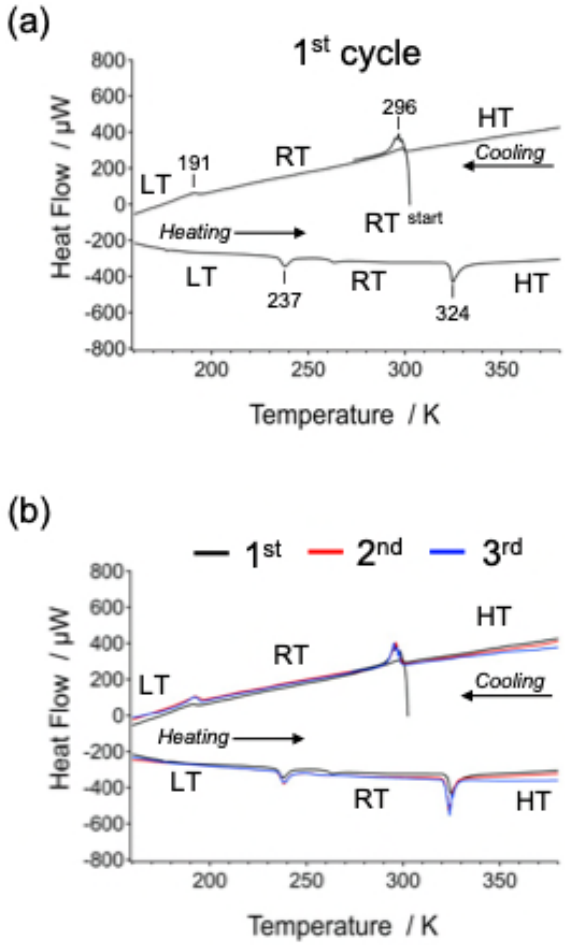

Fig. S4. (a) DSC profile recorded by heating and cooling of crystals **1**. (b) Comparison of the DSC profiles for 1st, 2nd, and 3rd measurements using the same specimen of **1**. The heating and cooling rates in all experiments were 5 K min^{-1}.

5. Optical properties of LT, RT, and HT

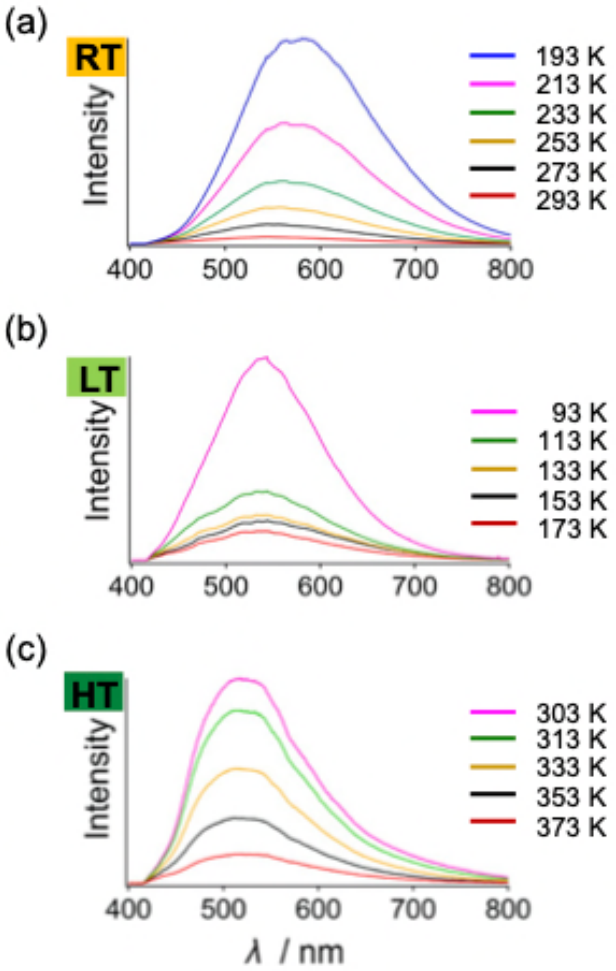

Fig. S5. Temperature-dependent photoluminescence spectra of (a) **RT** crystal recorded from 193 to 293 K, (b) **LT** crystal recorded from 93 to 173 K, and (c) **HT** crystal recorded from 303 to 373 K.

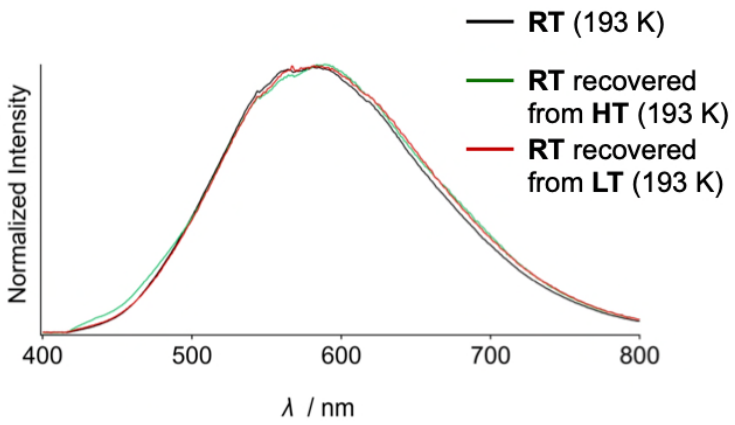

Fig. S6. Photoluminescence spectra of **RT** crystal recovered from **HT** and **LT** crystal (λ_{ex} = 365 nm).

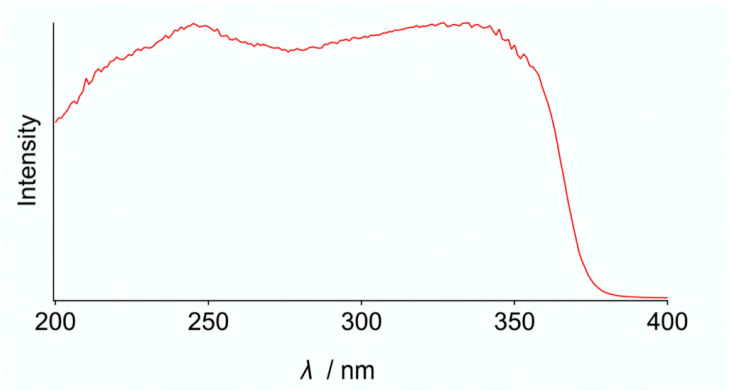

Fig. S7. Absorption spectrum of **RT** crystals at room temperature.

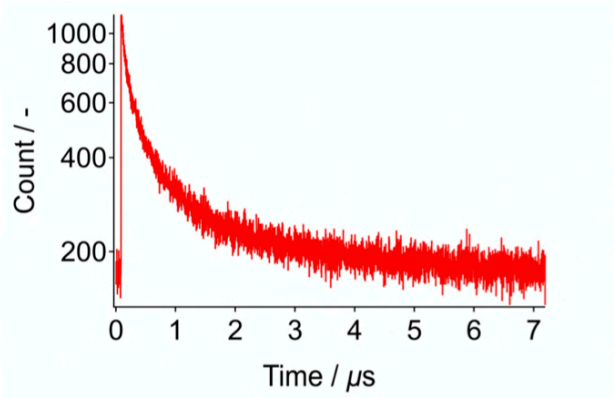

Fig. S8. Emission decay profile of **RT** (λ_{em} = 575 nm) under excitation at 371 nm.

Table S1. Photophysical properties of **RT** at room temperature.

	Φ_{em} / - (λ_{ex} / nm)	τ_{av} / μs[a,b] (λ_{em} / nm)	τ_1 / μs (A / -)	τ_2 / μs (A / -)	τ_3 / μs (A / -)
RT	0.007 (358)	2.05 (575)	0.46 (0.16)	0.09 (0.03)	2.43 (0.81)

[a] λ_{ex} = 371 nm. [b] $\tau_{av} = \Sigma \tau_n A_n$.

6. Single-crystal XRD structure analyses of LT, RT, and HT

Table S2. X-ray crystallographic data for **LT**, **RT**, and **HT**

compound	**LT**	**RT**	**HT**
CCDC Number	2081347	2081348	2081349
Empirical Formula	$C_{11}H_8AuBrF_4N_2$	$C_{11}H_8AuBrF_4N_2$	$C_{11}H_8AuBrF_4N_2$
Formula Weight	521.07	521.07	512.07
Crystal Size / mm	0.27×0.19×0.04	0.27×0.19×0.04	0.27×0.19×0.04
Crystal System	monoclinic	monoclinic	orthorhombic
a / Å	7.6850(3)	14.0862(6)	12.9752(7)
b / Å	15.3186(4)	15.4831(7)	6.8244(4)
c / Å	12.9425(5)	12.9171(5)	15.5938(10)
α / °	90	90	90
β / °	120.622(5)	106.586(4)	90
γ / °	90	90	90
V / Å^3	1311.16(10)	2700.0(2)	1380.80(14)
Space Group	$P2_1/c$	$P2_1/c$	$Pnma$
Z value	4	8	4
D_{calc} / g cm^{-3}	2.640	2.564	2.507
Temperature / K	123	293	363
$2\theta_{max}$ / °	58.822	58.898	58.486
μ / cm^{-1}	143.01 (Mo K$_\alpha$)	138.90 (Mo K$_\alpha$)	135.80 (Mo K$_\alpha$)
No. of Reflections	Total: 12804 Unique: 3100 R_{int}: 0.0382	Total: 35621 Unique: 6648 R_{int}: 0.0309	Total: 12492 Unique: 1812 (R_{int}: 0.0509)
R_1[a]; wR_2[b]	0.0212; 0.0523	0.0422; 0.1190	0.0387; 0.1187
GOF[c]	1.030	1.061	1.058
Max./Min. peak I[d] / Å^3	1.48 e$^-$/−1.15 e$^-$	3.11 e$^-$/−1.61 e$^-$	1.71 e$^-$/−1.49 e$^-$

[a]: For data with $I > 2.00\sigma(I)$. [b]: For all reflection data. [c]: Goodness of Fit.

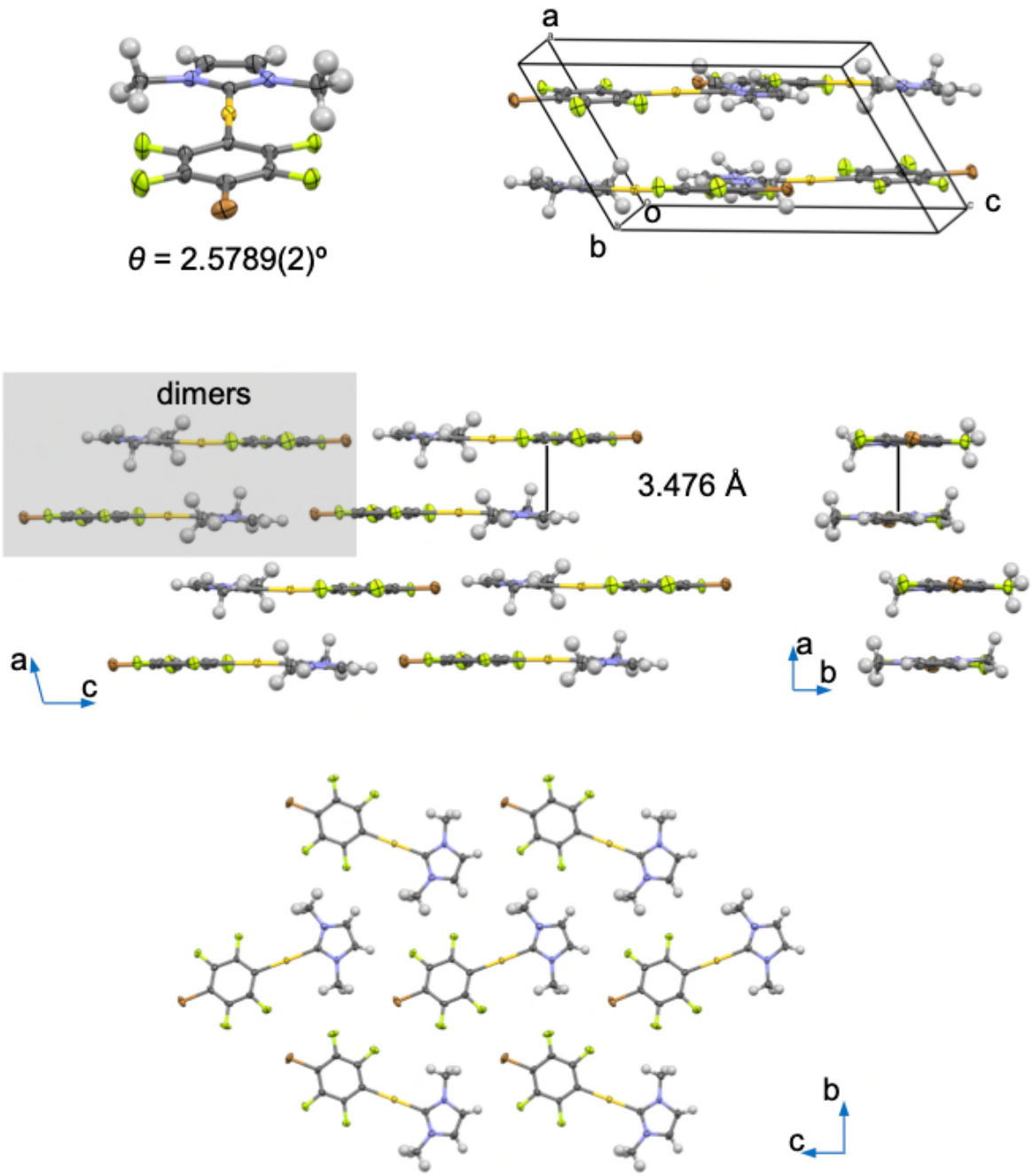

Fig. S9. Single-crystal structure of **LT** at 123 K.

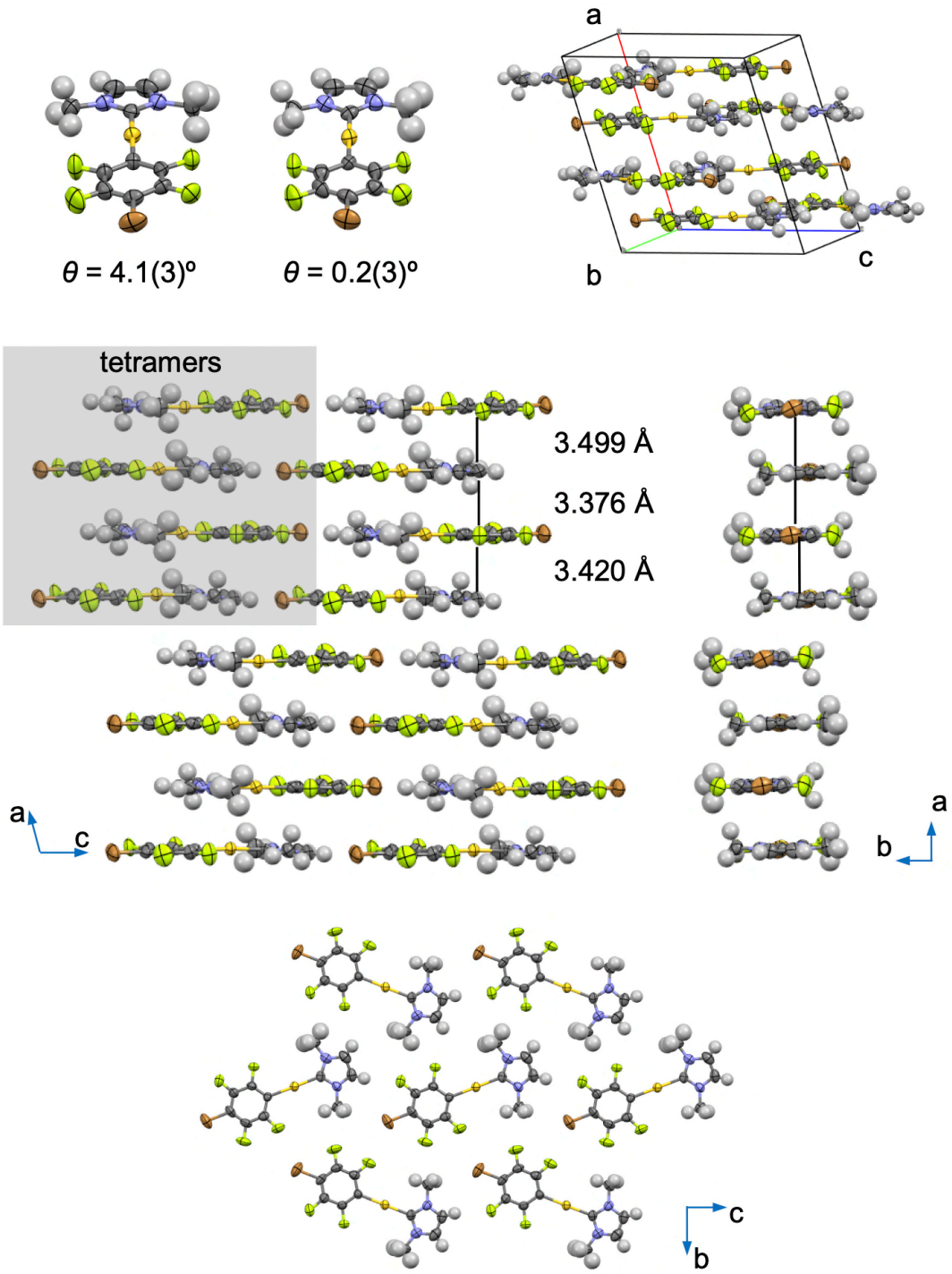

Fig. S10. Single-crystal structure of **RT** at 293 K.

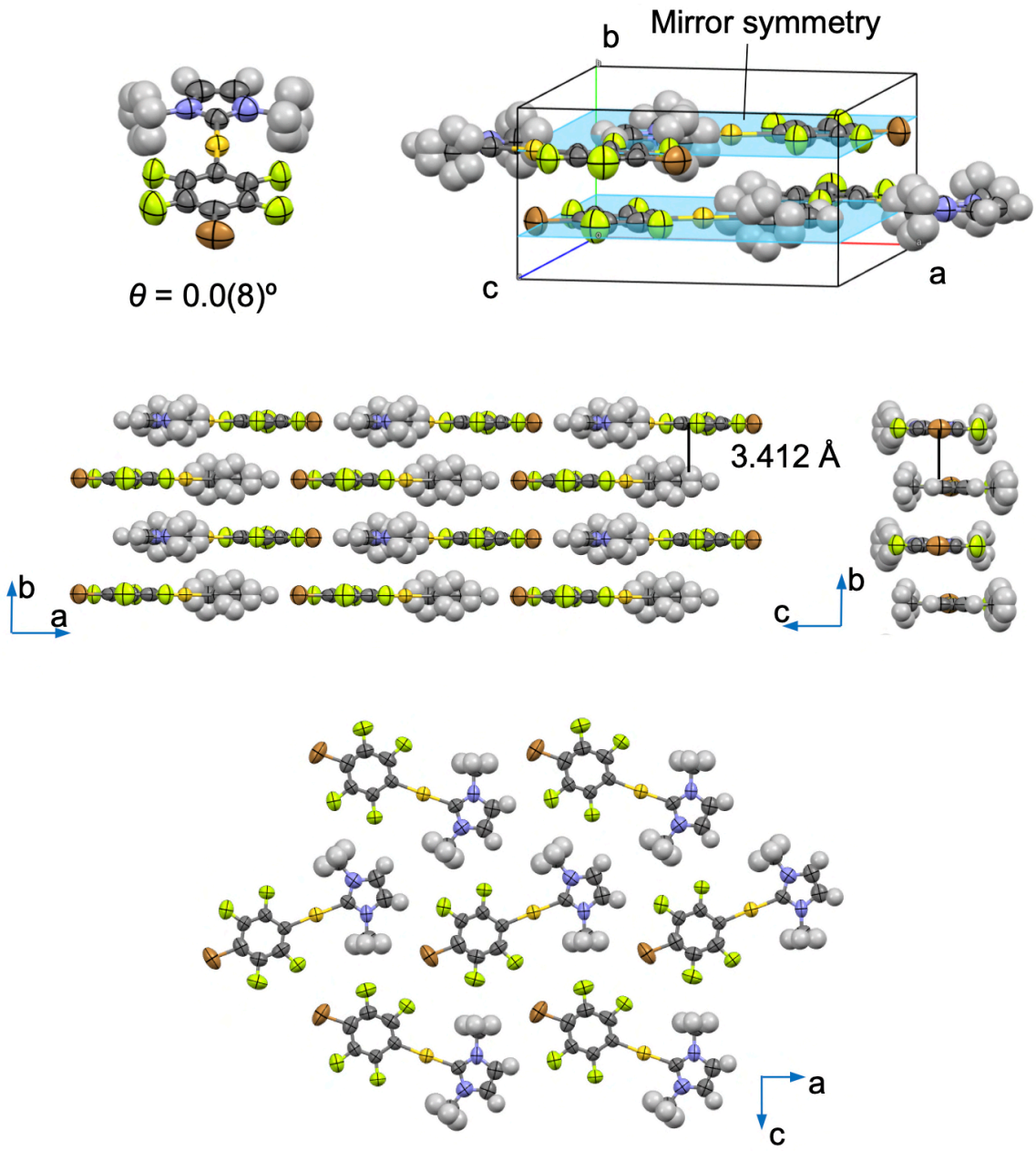

Fig. S11. Single-crystal structure of **HT** at 363 K. The modeled structure of the hydrogen looks rather complicated because the center of the molecule of **1** sits on the mirror plane.

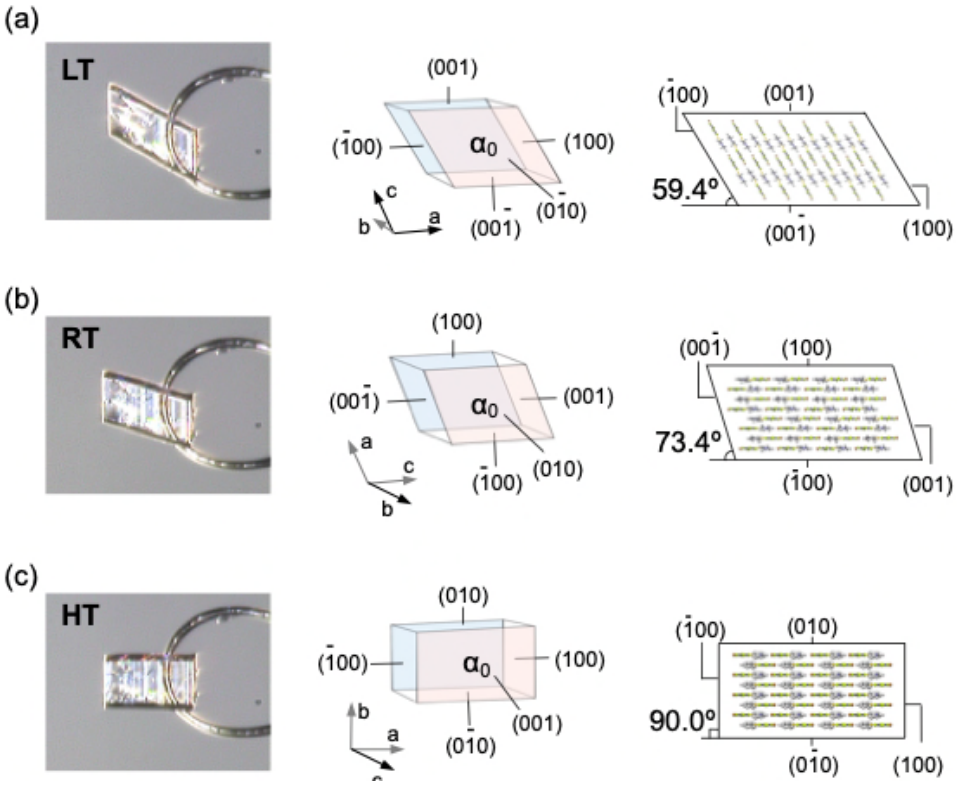

Fig. S12. Optical image and crystal packing with face indices of (a) the **LT** crystal at 123 K, (b) the **RT** crystal at 293 K, and (c) the **HT** crystal at 363 K.

7. Images and single-crystal XRD structure analyses of *b*-LT, *b*-RT, and *s*-HT

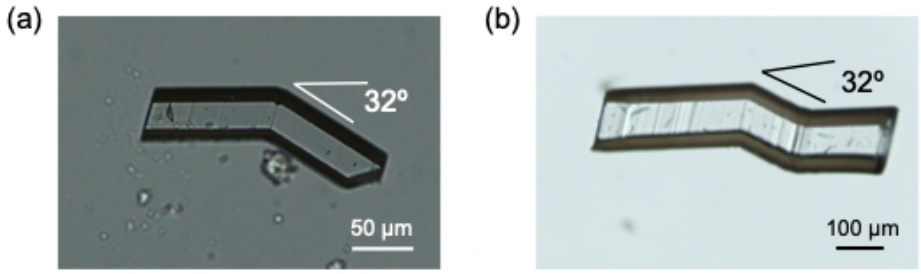

Fig. S13. Photographic images of ***b*-RT**.

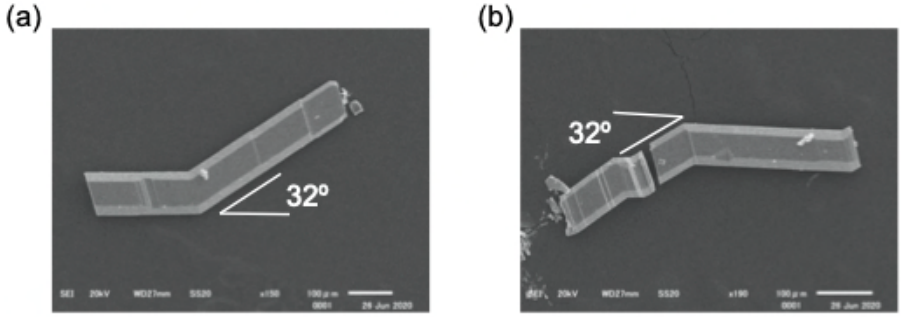

Fig. S14. SEM images of ***b*-RT**.

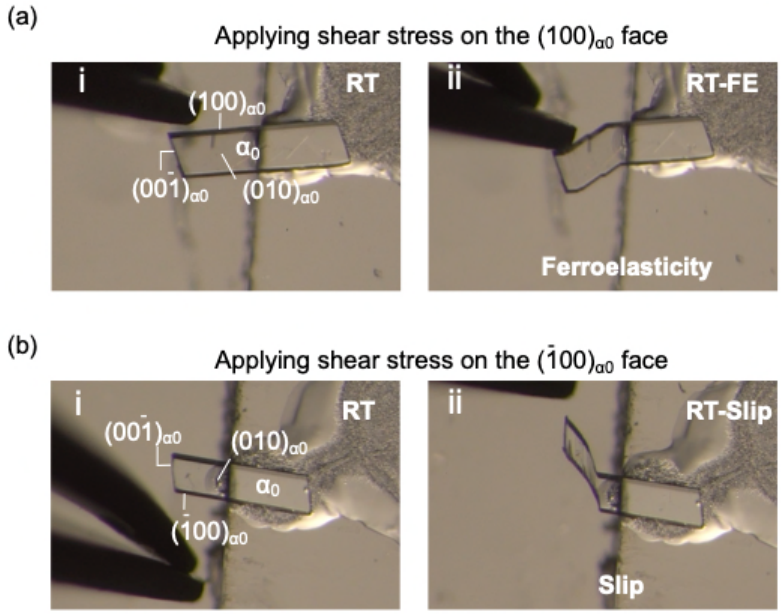

Fig. S15. Photographic images of deformed **RT**. The mechanical properties of the **RT** crystal were investigated by applying shear stress at the $(100)_{\alpha 0}$ face and $(-100)_{\alpha 0}$ face, which showed (a) ferroelastic and (b) slip deformation, respectively.

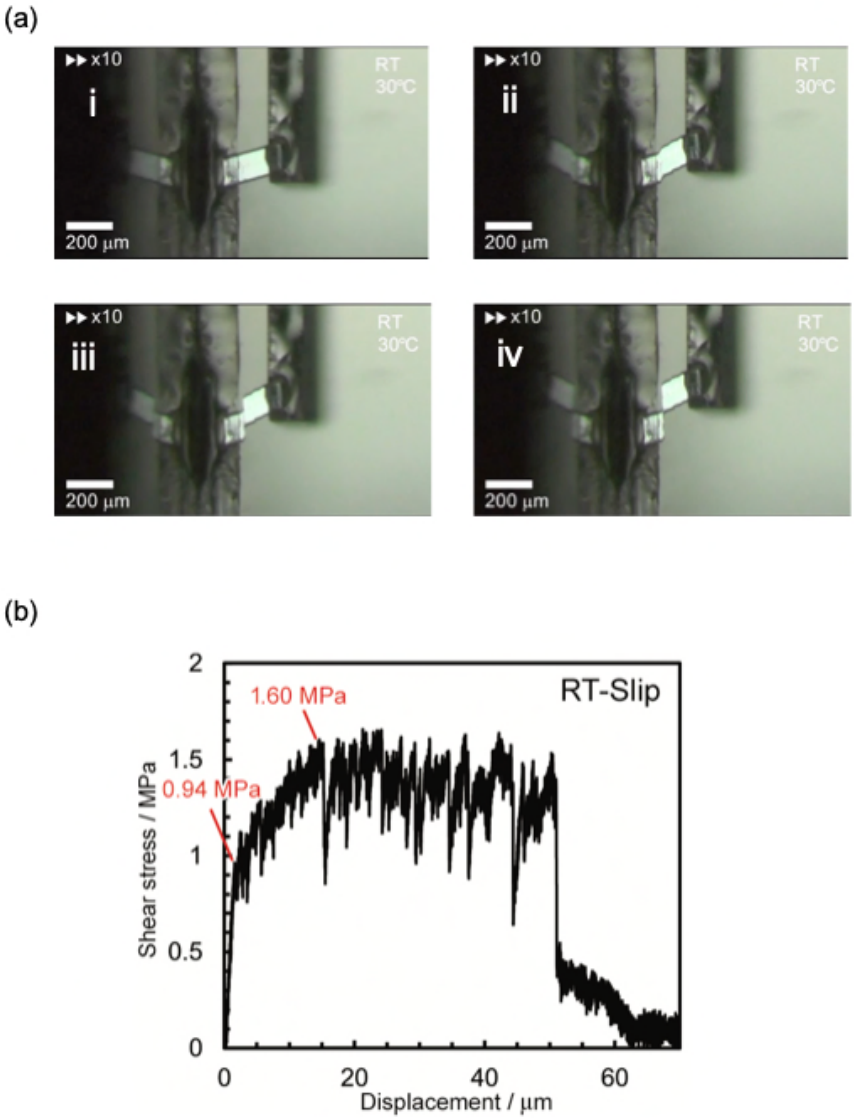

Fig. S16. (a) Snapshots of slip deformation of **RT** upon application of shear stress under visible light at 30 ºC. (b) Stress-displacement result of the crystal under VIS light.

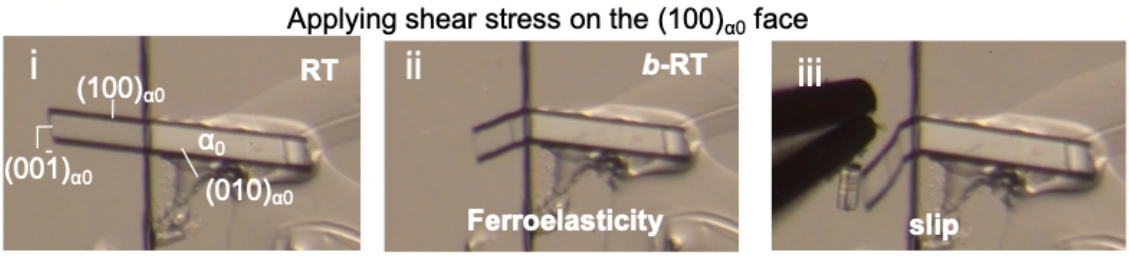

Fig. S17. Photographic images of a deformed **RT** crystal upon applying shear stress on the $(100)_{a0}$ face.

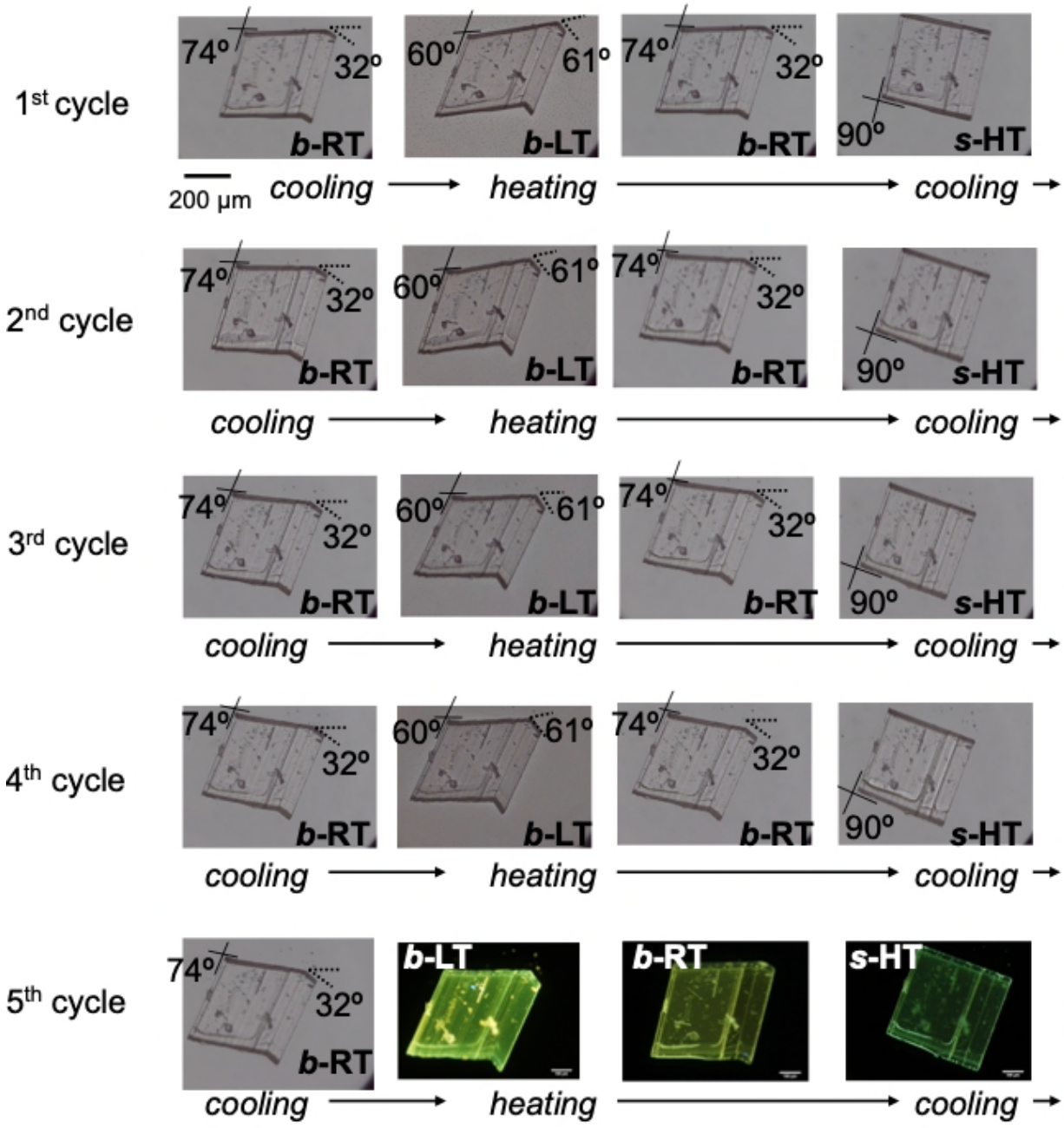

Fig. S18. Photographic images of reversible multi-stage shape-changing effect of ***b*-RT** upon heating/cooling at 20 K min^{-1}.

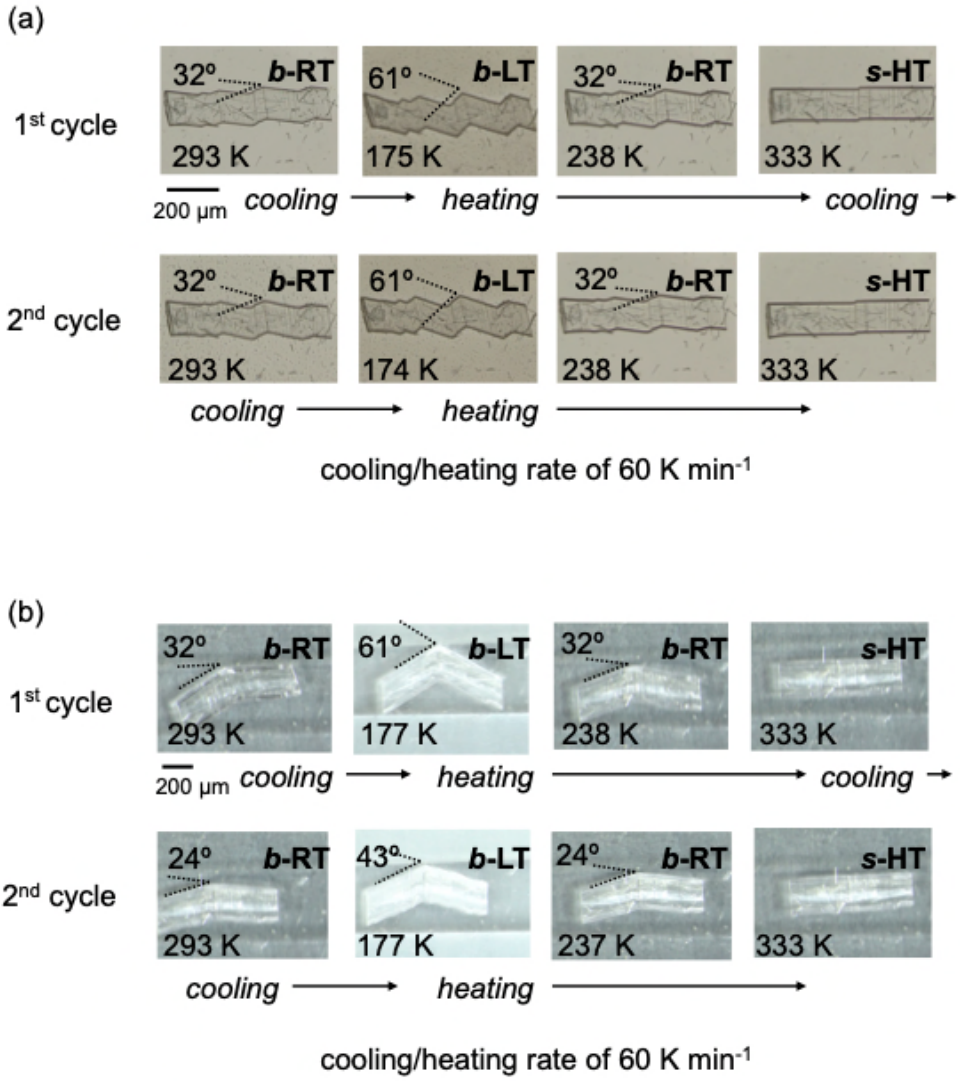

Fig. S19. Photographic images of reversible multi-stage shape-changing effect of ***b*-RT** upon heating/cooling at 60 K min^{-1}.

Table S3 X-ray crystallographic data for ***b*-LT**, ***b*-RT**, and ***s*-HT**

compound	***b*-LT**	***b*-RT**	***s*-HT**
CCDC Number	2081350	2081351	2081352
Empirical Formula	$C_{11}H_8AuBrF_4N_2$	$C_{11}H_8AuBrF_4N_2$	$C_{11}H_8AuBrF_4N_2$
Formula Weight	521.07	521.07	512.07
Crystal Size / mm	0.35×0.25×0.06	0.40×0.15×0.07	0.40×0.15×0.07
Crystal System	monoclinic	monoclinic	orthorhombic
a / Å	7.6985(5)	14.0976(5)	12.9715(6)
b / Å	15.3528(8)	15.4992(5)	6.8326(3)
c / Å	12.9738(8)	12.9484(4)	15.6063(8)
α / °	90	90	90
β / °	120.533(9)	106.584(4)	90
γ / °	90	90	90
V / Å^3	1320.79(17)	2711.55(16)	1383.17(11)
Space Group	$P2_1/c$	$P2_1/c$	Pnma
Z value	4	8	4
D_{calc} / g cm^{-3}	2.620	2.553	2.502
Temperature / K	123	293	363
$2\theta_{max}$ / °	56.752	59.006	58.126
μ / cm^{-1}	141.79 (Mo K$_\alpha$)	138.30 (Mo K$_\alpha$)	135.80 (Mo K$_\alpha$)
No. of Reflections	Total: 5301 Unique: N/A[a] (R_{int}: N/A[a])	Total: 12298 Unique: N/A[a] (R_{int}: N/A[a])	Total: 12492 Unique: 1812 (R_{int}: 0.0509)
R_1[b]; wR_2[c]	0.0714; 0.2239	0.0836; 0.2241	0.0387; 0.1187
GOF[d]	1.050	1.039	1.058
Max./Min. peak I[d] / Å^3	4.55 e$^-$/−3.38 e$^-$	1.81 e$^-$/−1.58 e$^-$	1.71 e$^-$/−1.49 e$^-$

[a]: Not available because of the twin analyses. [b]: For data with $I > 2.00\sigma(I)$. [c]: For all reflection data. [d]: Goodness of Fit.

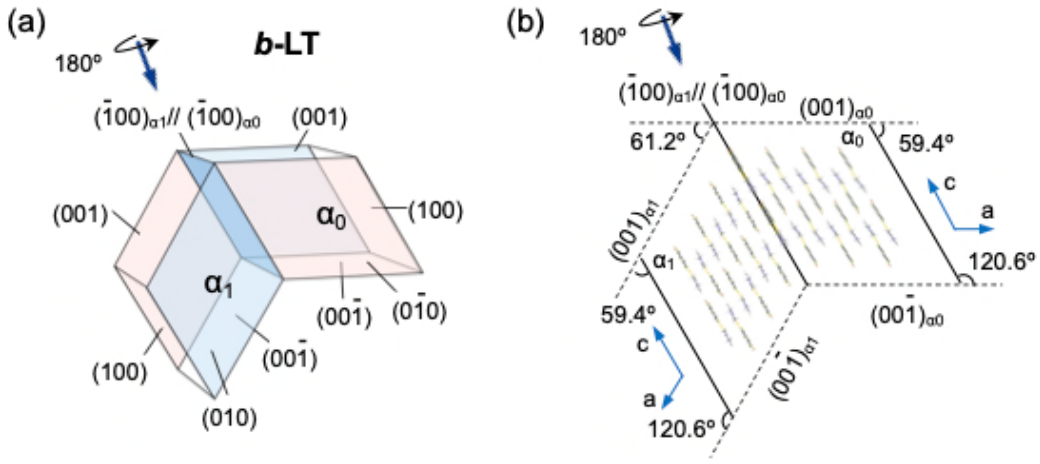

Fig. S20. The crystal face indices and packing arrangements of ***b*-LT**.

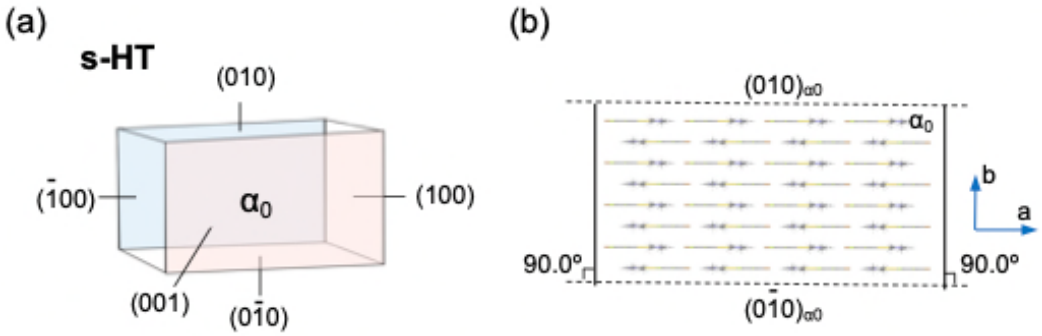

Fig. S21. The crystal face indices and packing arrangements of ***s*-HT**.

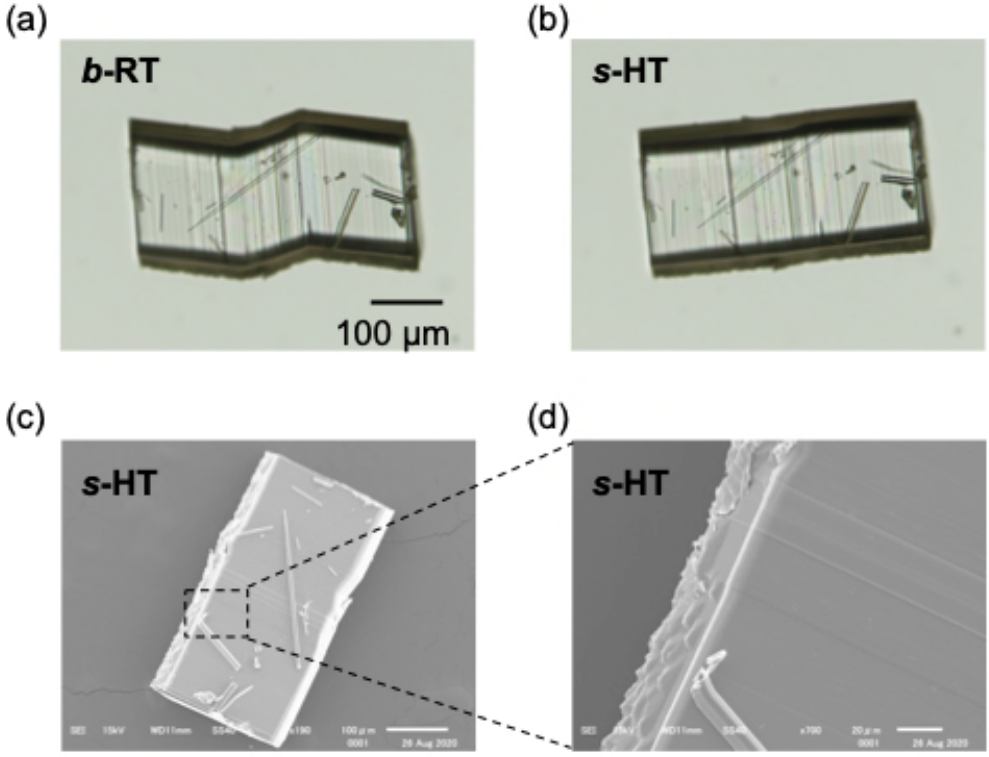

Fig. S22. Photographs of ***b*-RT** upon heating to recover the original straight shape through the phase transition into ***s*-HT**. (a, b) Photographic image of ***b*-RT** and ***s*-HT**. (c, d) SEM images of ***s*-HT**.

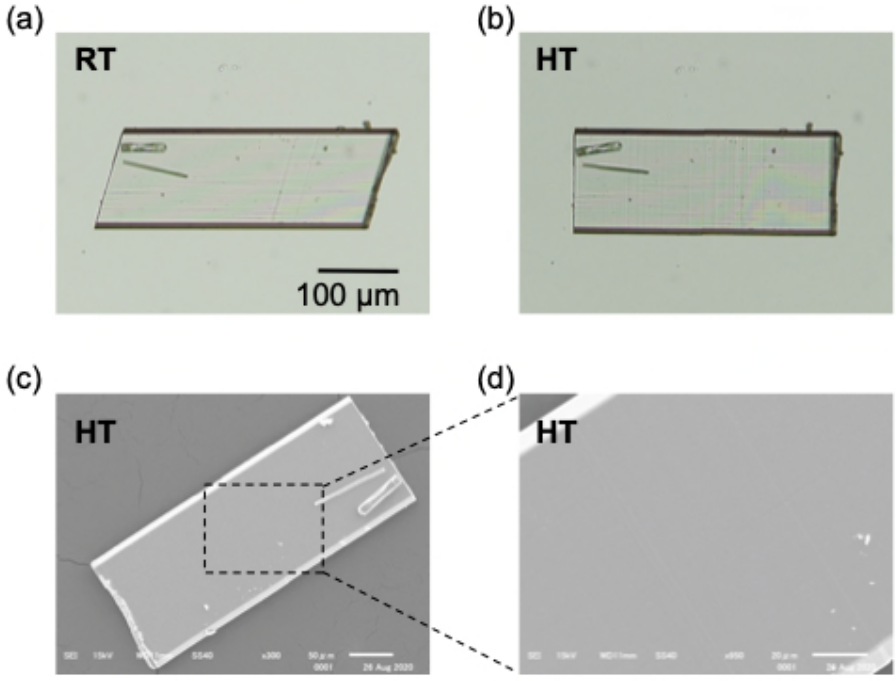

Fig. S23. A crystal **RT** transformed into **HT** upon heating. (a, b) Photographic images of **RT** and **HT**. (c, d) SEM images of **HT**.

8. NMR spectra

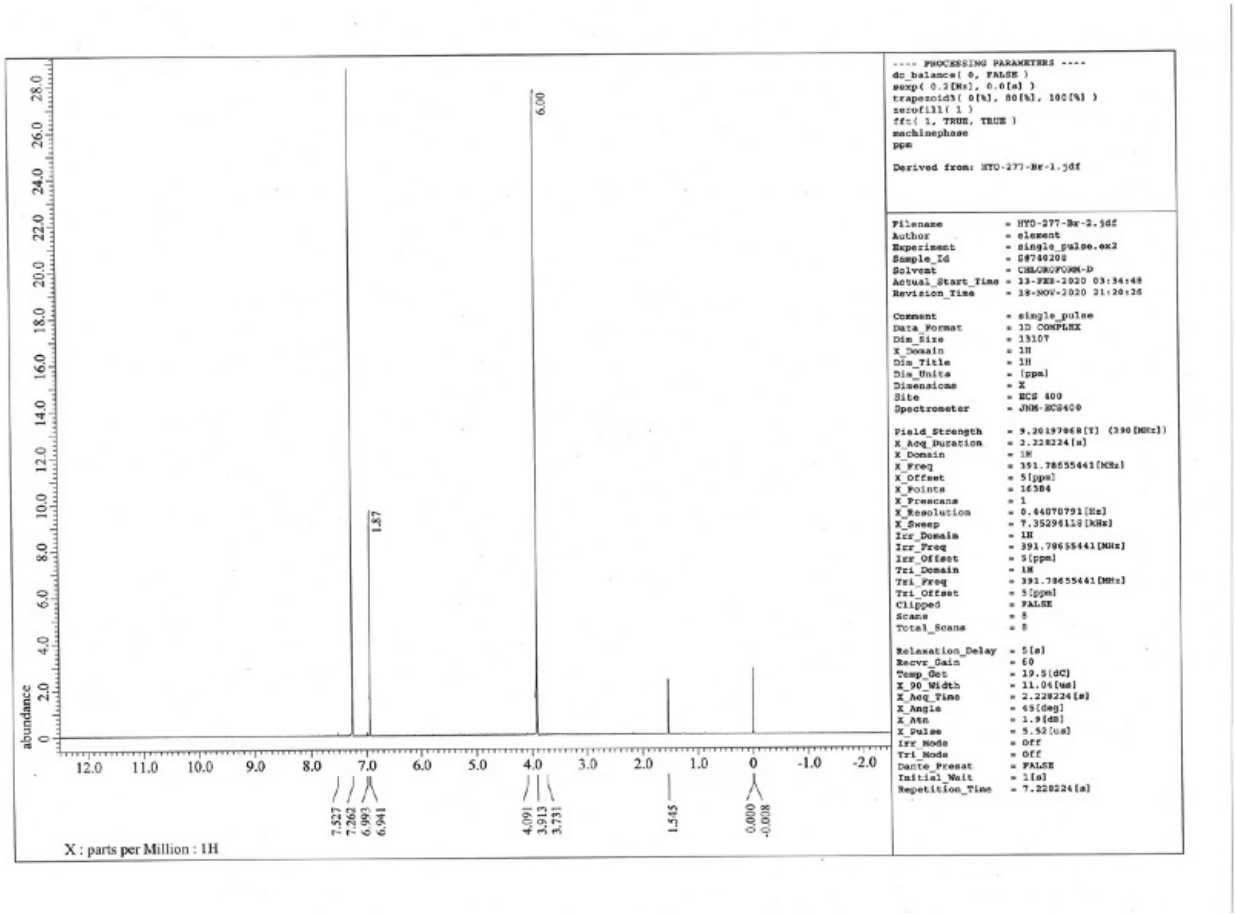

Fig. S24 ^{1}H NMR spectrum of **1** in $CDCl_3$.

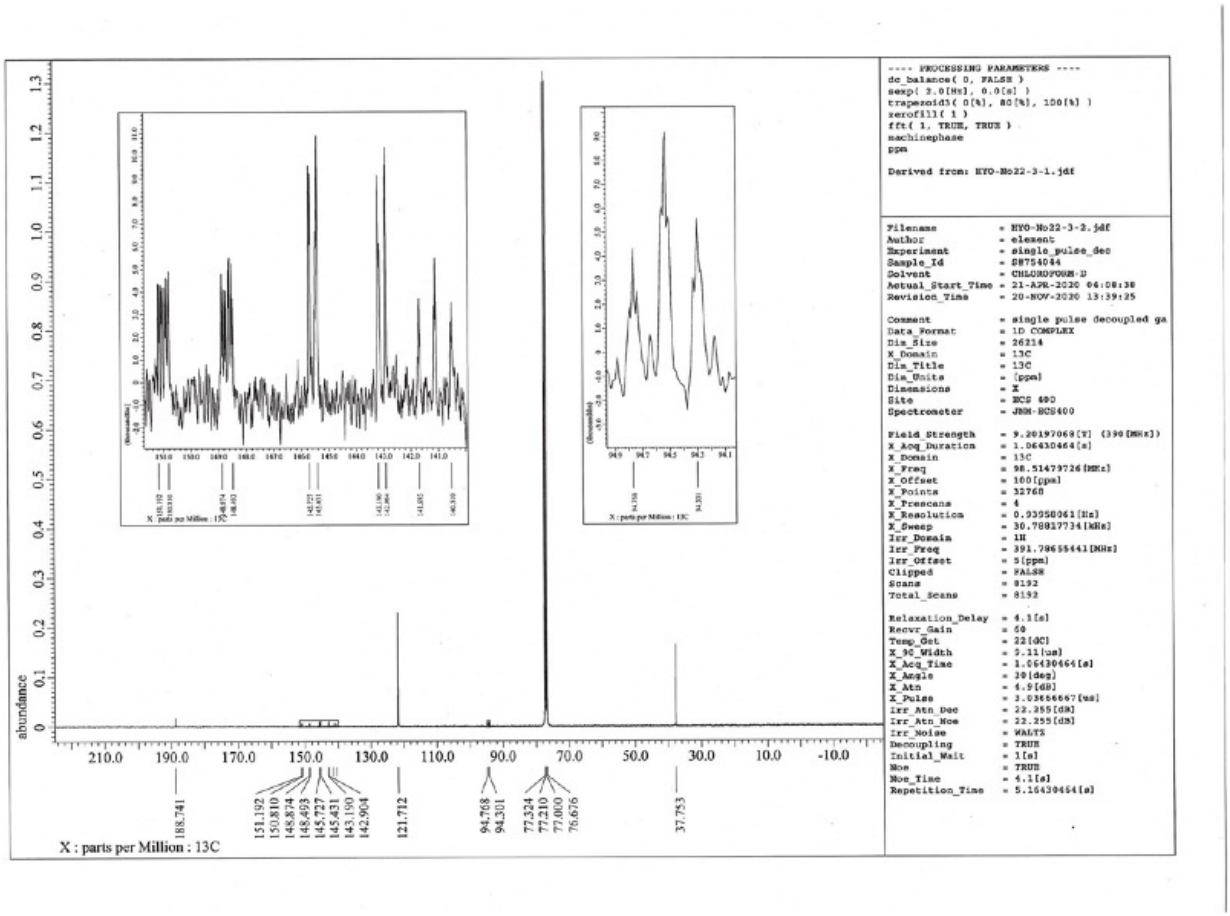

Fig. S25 ^{13}C NMR spectrum of **1** in $CDCl_3$.

9. References

S1. Sheldrick, G. M. SHTLXT - Integrated space-group and crystal-structure determination. *Acta Cryst.* **2015**, *A71*, 3–8.

S2. Sheldrick, G. M. Crystal structure refinement with SHELXL. *Acta Cryst.* **2015**, *C71*, 3–8.

S3. Dolomanov, O. V.; Bourhis, L. J.; Gildea, R. J.; Howard, J. A. K.; Puschmann, H. OLEX2: a complete structure solution, refinement and analysis program. *J. Appl. Crystallogr.* **2009**, *42*, 339–341.

S4. A. Johnson M. C. Gimeno, *Chem. Commun*. **2016**, *52*, 9664–9667.

S5. Bayón, B.; Coco, S.; Espinet, P.; Fernández-Mayordomo, C.; Martín-Alvarez, J. M. *Inorg. Chem.* **1997**, *36*, 2329–2334.